Lecture 7. More on BL wind profiles and turbulent eddy structures

In this lecture…

- Stability and baroclinicity effects on PBL wind and temperature profiles
- Large-eddy structures and entrainment in shear-driven and convective BLs.

Stability effects on overall boundary layer structure

Above the surface layer, the wind profile is also affected by stability. As we mentioned previously, unstable BLs tend to have much more well-mixed wind profiles than stable BLs. Fig. 1 shows observations from the Wangara experiment on how the velocity defects and temperature profile are altered by BL stability (as measured by H/L). Within stability classes, the velocity profiles collapse when scaled with a velocity scale u_* and the observed BL depth H, but there is a large difference between the stability classes.

Baroclinicity

We would expect baroclinicity (vertical shear of geostrophic wind) to also affect the observed wind profile. This is most easily seen for a laminar steady-state Ekman layer in a geostrophic wind with constant vertical shear $\mathbf{u}_g(z) = (G + Mz, Nz)$, where $M = -(g/fT_0)\partial T/\partial y$, $N = (g/fT_0)\partial T/\partial x$. The momentum equations and BCs are:

$$-f(v - Nz) = \nu\, d^2u/dz^2$$

$$f(u - G - Mz) = \nu\, d^2v/dz^2$$

$$u(0) = 0,\ u(z) \sim G + Mz \text{ as } z \to \infty.$$

$$v(0) = 0,\ v(z) \sim Nz \text{ as } z \to \infty.$$

The resultant BL velocity profile is the classical Ekman layer with the thermal wind added onto it.

$$u(z) = G(1 - e^{-\zeta} \cos \zeta) + Mz, \tag{7.1}$$

$$v(z) = G\, e^{-\zeta} \sin \zeta + Nz. \quad (\zeta = z/\delta_E,\ \delta_E = (2\nu/f)^{1/2}) \tag{7.2}$$

The added linear shear drives a height-independent viscous momentum flux which affects the surface stress but does not perturb the vertical convergence of the momentum flux.

The added contribution of the thermal wind can considerably alter the BL wind profile. Fig. 7.2 shows example wind hodographs with $M = 0$ and N positive, zero, and negative. The near-surface wind is slightly more turned toward the surface low pressure to the north. The largest crossing angle of the surface wind direction across the surface isobars (aligned along the x-axis) occurs if $M < 0, N > 0$, corresponding to surface cold advection. This effect is clearly seen in Fig. 7.3, showing average crossing angle vs. thermal wind orientation in 23000 wind profiles over land (Hoxit 1974). On weather maps, one can see much larger crossing angles behind cold fronts than ahead of them. On the other hand, the wind turns less with height if $N > 0$ (surface cold advection). The effect is stronger in the late afternoon (00Z) than the early morning (12Z) soundings. This is because during the day, convection allows more vigorous mixing of air from significant height down close to the surface, allowing the thermal wind to have a stronger effect.

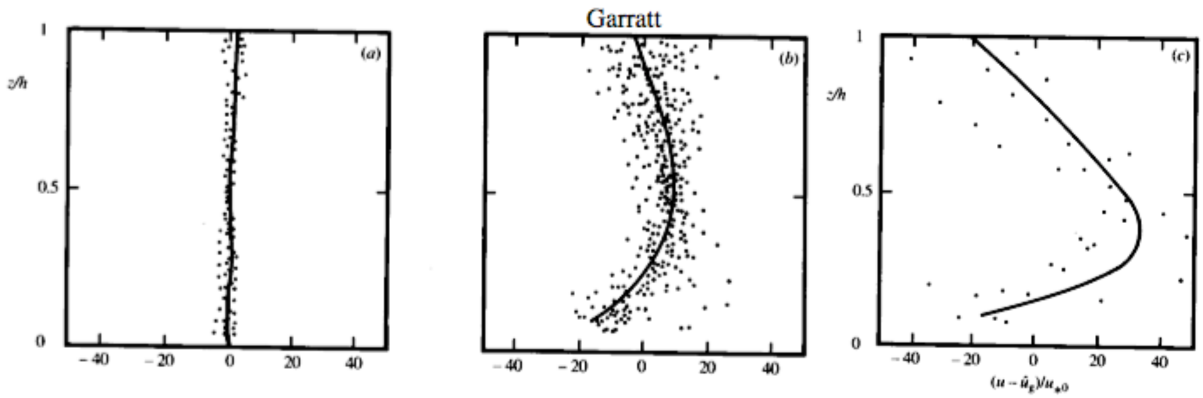

Fig. 3.13 Profiles of the normalized velocity defect for the u-component as a function of normalized height z/h, based on Eq. 3.82 and an analysis of Wangara observations. Three stability regimes are presented: (a) $-150 < h/L < -120$; (b) $0 < h < 30$; (c) $180 < h/L < 210$. Curves are drawn by eye. After Yamada (1976), *Journal of Atmospheric Sciences*, American Meteorological Society.

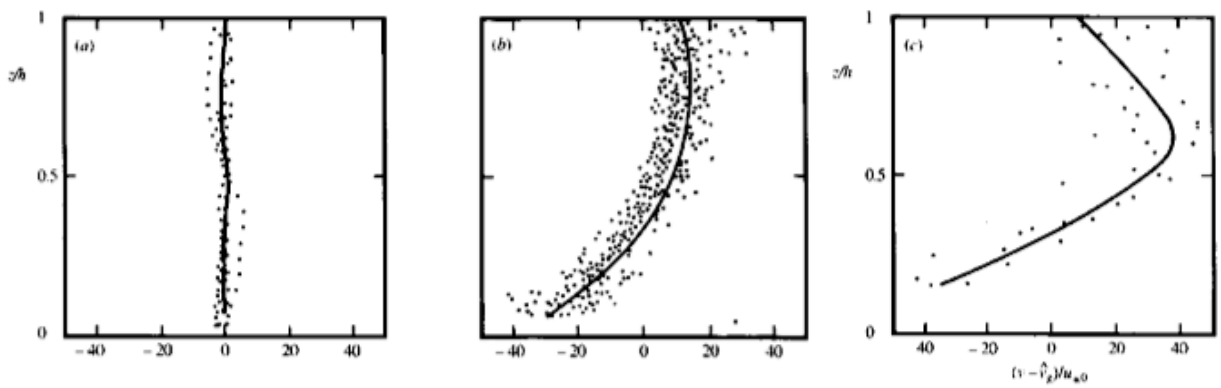

As above, except for v.

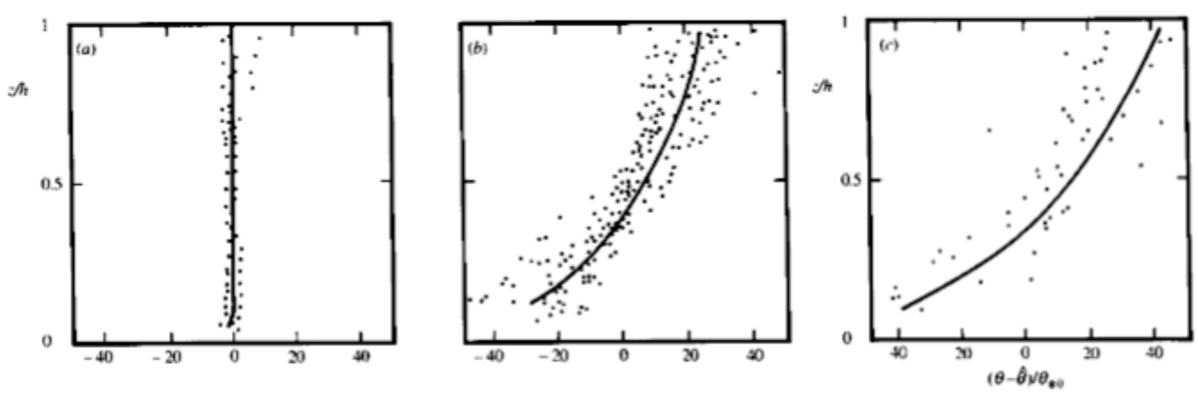

As above, except for θ. Here $\hat{\theta}$ is the BL-mean θ.

Fig. 7.1: Scaled ageostrophic velocity and potential temperature profiles in convective (h/L << 0), neutral ($h/L \approx 0$) and unstable (h/L >> 0) boundary layers. Here h (H in text) is the BL depth and L the Obukhov length. Note relative well-mixedness of the unstable profiles.

Sorbjan

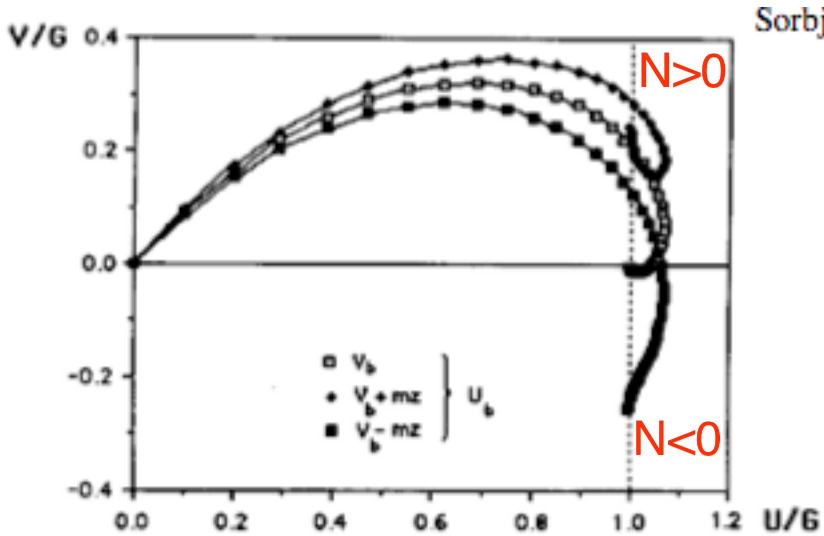

Figure 6.11 Ekman spirals obtained for the baroclinic correction of the V component of the wind velocity, $a = 0.001$, $m = 0.0001$. Points are plotted every 100 m, starting on the surface. U_b, V_b-barotropic components of the wind vector. Dotted line shows directions of the thermal wind vectors.

Fig. 7.2: Ekman spirals for thermal wind with $M = 0$ and $N > 0$, $N = 0$ (no thermal wind), $N < 0$. Near-surface wind is oriented more in $+y$ direction (larger crossing angle) for $N > 0$.

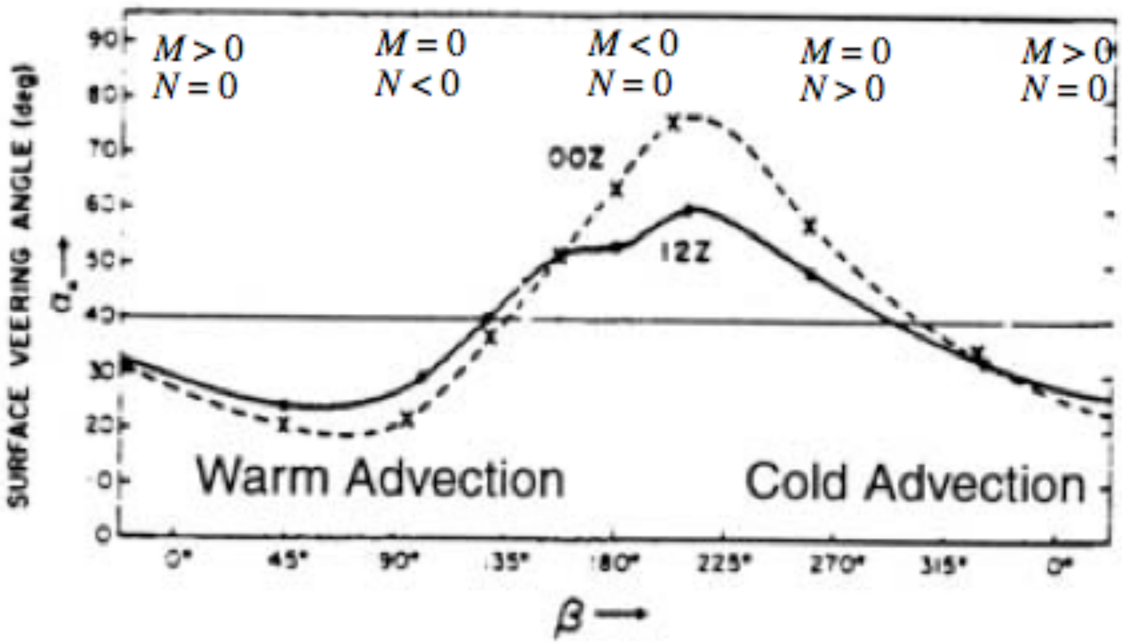

Fig. 7.3: Isobaric crossing angle of surface wind vs. angle of thermal wind. Afternoon (00 Z) soundings show stronger effect due to stronger vertical mixing in a more convective BL (Hoxit 1974).

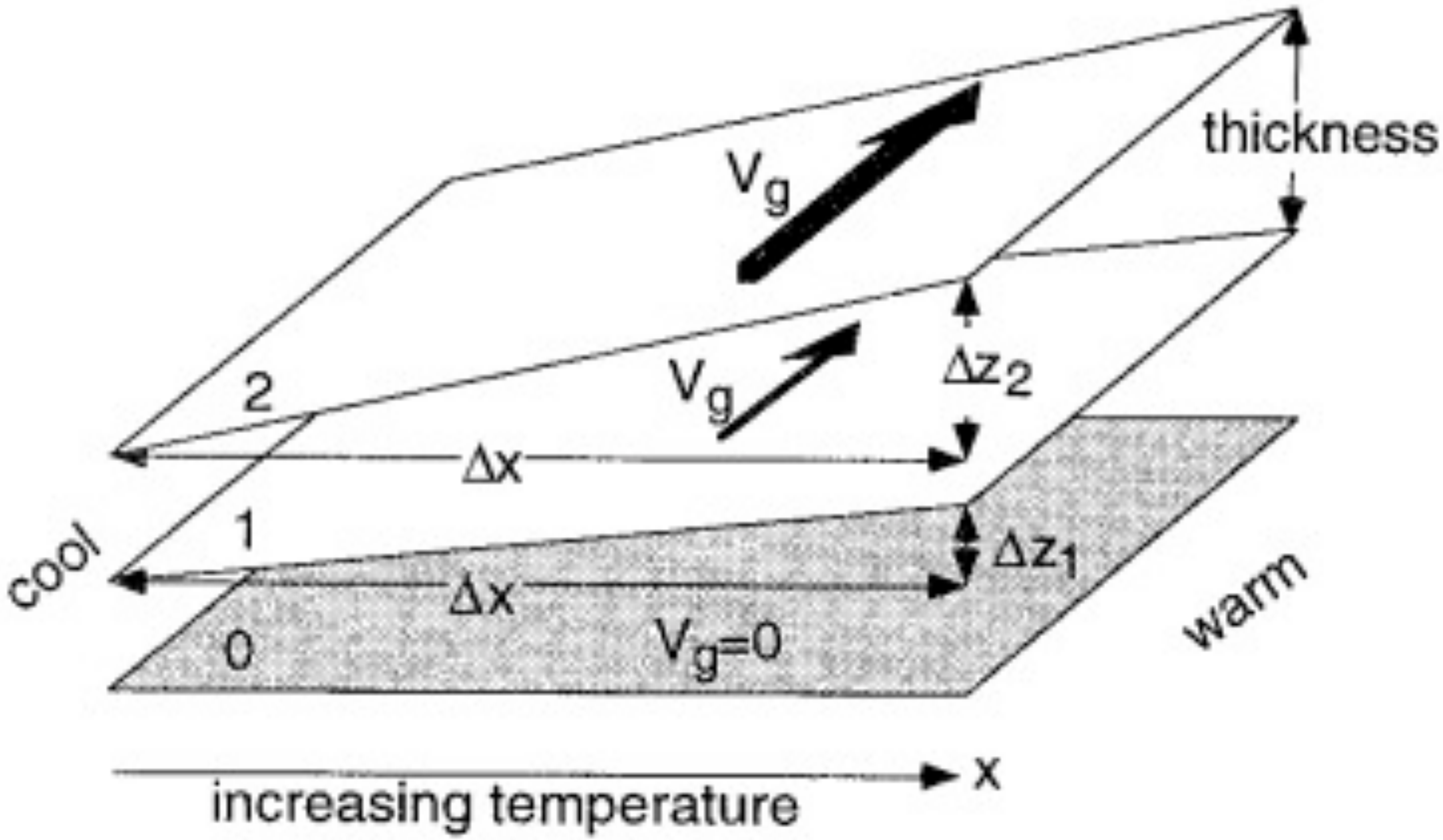

Figure 11.7

The three planes are surfaces of constant pressure (i.e., isobaric surfaces). Surface #2 has lower pressure than surface #1, etc. A horizontal temperature gradient tilts the pressure surfaces and causes the geostrophic wind to increase with height.

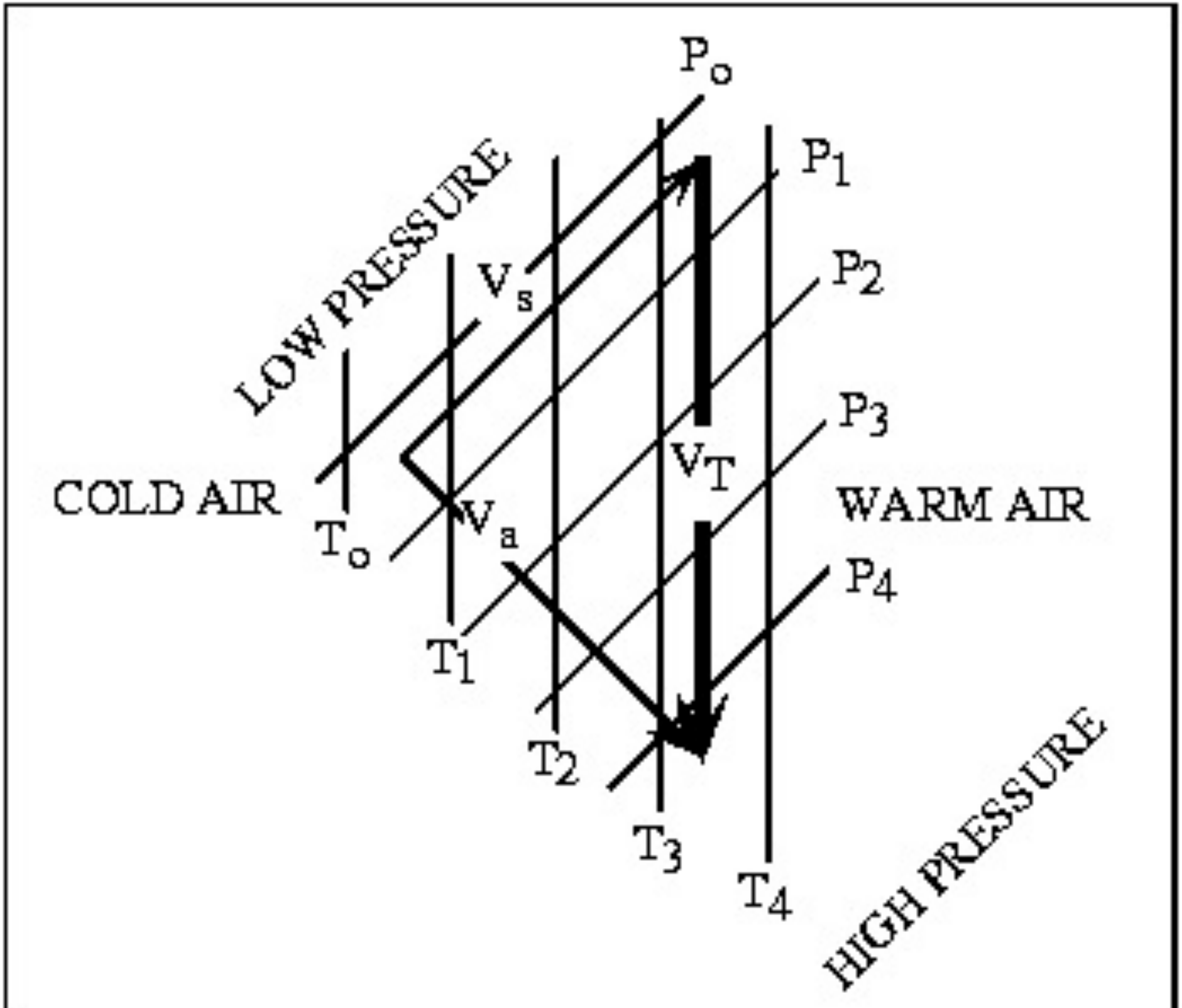

P_o
P_1
P_2
P_3
P_4
LOW PRESSURE
V_s
V_T
V_a
COLD AIR
WARM AIR
T_o
T_1
T_2
T_3
T_4
HIGH PRESSURE

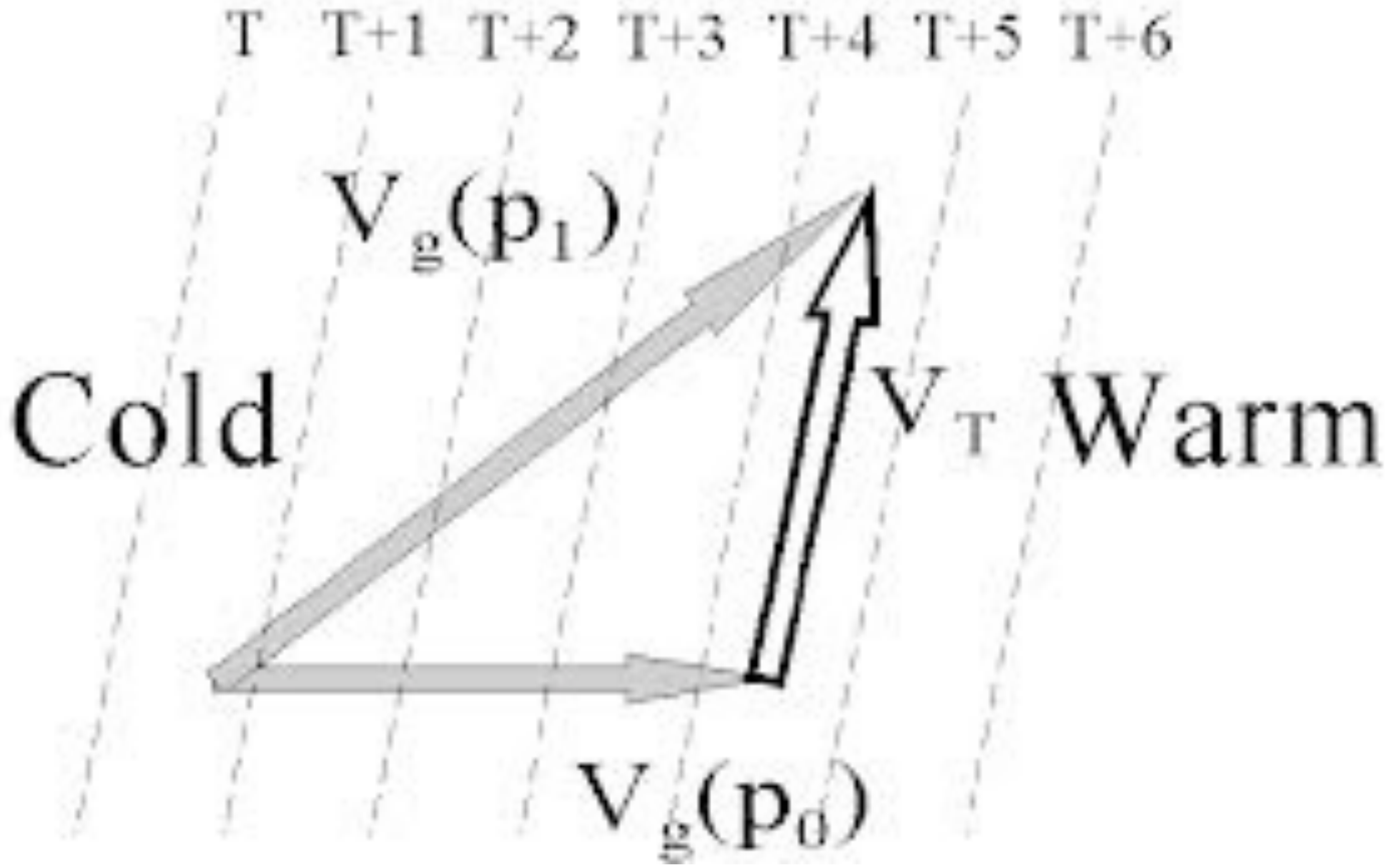

T
T+1
T+2
T+3
T+4
T+5
T+6
$V_g(p_1)$
Cold
V_T
Warm
$V_g(p_0)$

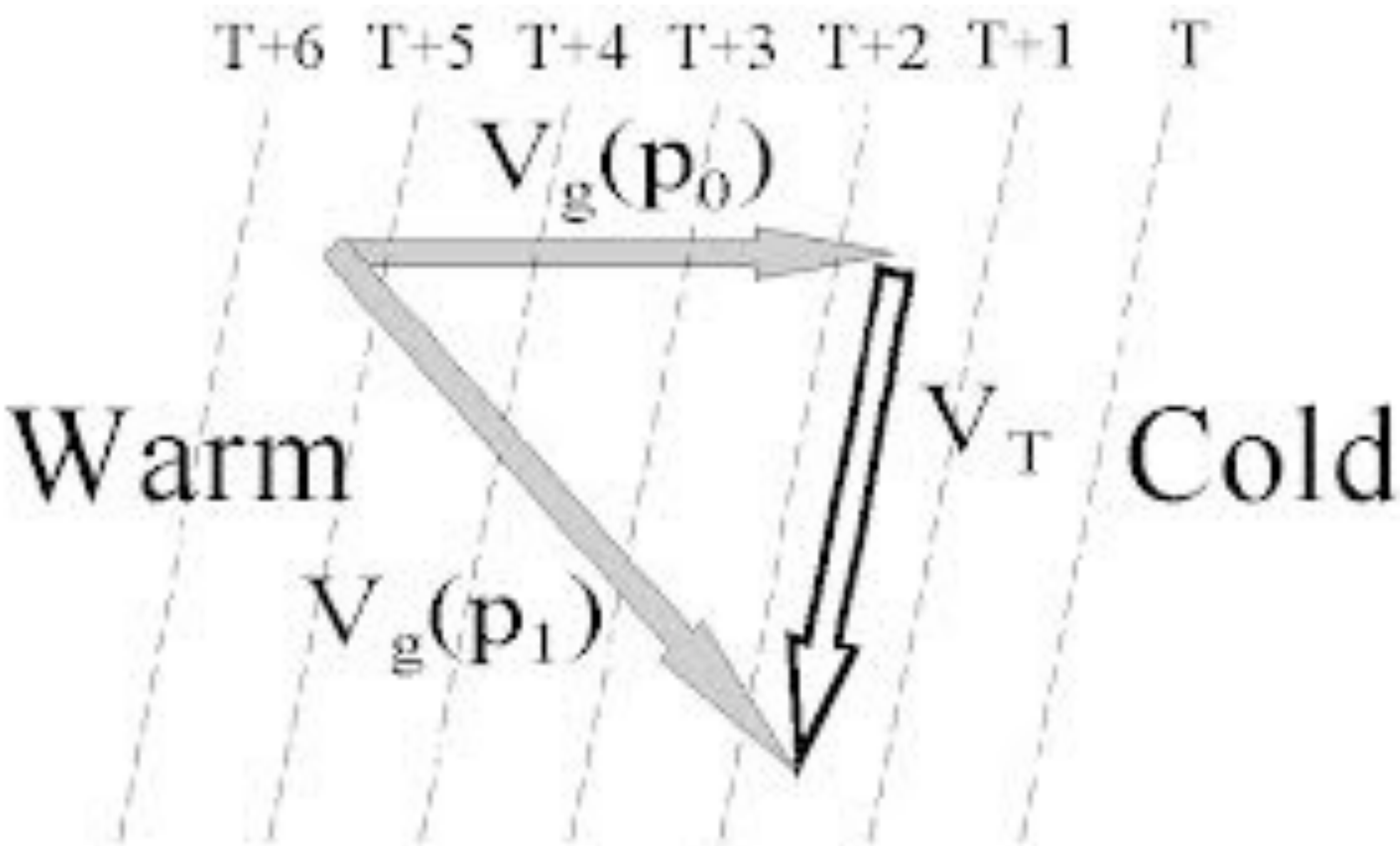
T+6
T+5
T+4
T+3
T+2
T+1
T
$V_g(p_0)$
Warm
V_T
Cold
$V_g(p_1)$